MiR-550a-3p restores damaged vascular smooth muscle cells by inhibiting thrombomodulin in an *in vitro* atherosclerosis model

Shiyuan Chen,[1,2] Longfei Zhang,[2] Benchi Feng,[2] Wei Wang,[3] Delang Liu,[2] Xinyu Zhao,[2] Chaowen Yu,[2] Xiaogao Wang,[2] Yong Gao[1,2]

[1]The First Clinical College, Jinan University, Guangzhou, Guangdong
[2]Department of Vascular Surgery, The First Affiliated Hospital of Bengbu Medical College, Bengbu, Anhui
[3]Department of Oncological Surgery, The Second Affiliated Hospital of Bengbu Medical College, Bengbu, Anhui, China

ABSTRACT

Thrombomodulin (TM) is involved in the pathological process of atherosclerosis; however, the underlying mechanism remains unclear. Oxidised low-density lipoprotein (Ox-LDL; 100 μg/mL) was used to induce human vascular smooth muscle cells (HVSMCs) into a stable atherosclerotic cell model. The expression levels of miR-550a-3p and TM were detected by real-time reverse transcription-polymerase chain reaction. Cell proliferation was estimated using CCK8 and EDU assays. Wound scratch and transwell assays were used to measure the ability of cells to invade and migrate. Propidium iodide fluorescence-activated cell sorting was used to detect apoptosis and cell cycle changes. A dual-luciferase reporter assay was performed to determine the binding of miR-550a-3p to TM. Our results suggested the successful development of a cellular atherosclerosis model. Our data revealed that TM overexpression significantly promoted the proliferation, invasion, migration, and apoptosis of HVSMCs as well as cell cycle changes. Upregulation of miR-550a-3p inhibited the growth and metastasis of HVSMCs. Furthermore, miR-550a-3p was confirmed to be a direct target of TM. Restoration of miR-550a-3p expression rescued the effects of TM overexpression. Thus, miR-550a-3p might play a role in atherosclerosis and, for the first time, normalised the function of injured vascular endothelial cells by simultaneous transfection of TM and miR-550a-3p. These results suggest that the miR-550a-3p/TM axis is a potential therapeutic target for atherosclerosis.

Key words: Thrombomodulin; atherosclerosis; miR-550a-3p.

Correspondence: Dr. Yong Gao, The First Clinical College, Jinan University; Department of Vascular Surgery, The First Affiliated Hospital of Bengbu Medical College, Bengbu, Anhui, China. E-mail: Dr.gaoyong@qq.com

Contributions: YG, study concept and design; SC, experiment performing, original manuscript drafting; LZ, data analysis, literature searching; BF, contribution to data analysis; WW, DL, results interpretation and discussion; XZ, CY, contribution to cell culture; XW, SC, YG, manuscript revision. All the authors read and approved the final version of the manuscript and agreed to be accountable for all aspects of the work.

Conflict of interest: The authors declare that they have no competing interests, and all authors confirm accuracy.

Ethics approval: The experimental protocols were approved by the Ethics Committee of the First Affiliated Hospital of Bengbu Medical College.

Data availability: The data used to support the findings of this study are available from the corresponding author upon request.

Funding: This study was supported by the Key Project of Natural Science research in Universities of Anhui Province (grant number: KJ2020A0558); the Key Project of Natural Science research in Universities of Anhui Province (grant number: KJ2021A0721); the post-graduate project of Natural Science research in Universities of Anhui Province (grant number: YJS2021A0538) and the key Scientific research project of Anhui Provincial Health Commission (grant number: AHWJ2021a016).

Introduction

Cardiovascular disease is the leading cause of death worldwide, and atherosclerosis is the primary cause of vascular diseases.[1,2] Atherosclerosis is generally considered a lipid storage disease.[3] Atherosclerosis involves a series of cellular and molecular events, including immune-inflammatory responses, recruitment and adhesion of leukocytes, and proliferation and migration of vascular smooth muscle cells.[4-7] The migration and proliferation of vascular smooth muscle cells and immune-inflammatory responses are vital pathophysiological steps in atherosclerosis. Some studies have reported that thrombomodulin (TM) protein might play a role in atherosclerosis through the above pathways.[8-10]

TM, a thrombin receptor, is primarily located on the surface of endothelial cells.[11] Soluble TM can be detected in the circulating plasma following endothelial surface proteolysis and is considered a marker of endothelial function.[12,13] TM has haemostatic and anti-inflammatory effects and regulates endothelial cell proliferation.[14] TM combines with thrombin to efficiently catalyse the production of activated protein C (APC).[15] APC, a clinically important endogenous anticoagulant, reduces coagulation by proteolytically inactivating factors Va and VIIIa.[16,17] Furthermore, APC inhibits endothelial inflammation and cell death pathways by binding to protease-activated receptor 1 or endothelin C receptor 4.[18-20] Notably, TM can also directly activate anti-inflammatory pathways through its N-terminal lectin domain, negatively regulate complement, or promote the activation of thrombin-activated fibrinolysis inhibitors.[21,22] Therefore, the physiological significance of TM expression in muscle cells requires further investigation.

Laszik *et al*.[23] examined TM expression levels in six patients with severe coronary atherosclerosis. The results showed that the expression of TM on vascular endothelial cells of patients with severe coronary atherosclerosis was significantly reduced. One possible mechanism is the local loss of TM in endothelial cells, resulting in the focal injury of protein C activation, formation of a prethrombotic surface, and promotion of leukocyte influx into the arterial wall. Tohda *et al*.[24] demonstrated that recombinant TMD2 enhances mitogen activation and phosphorylation of protein kinases in smooth muscle cells and significantly increases the proliferation of rat vascular smooth muscle cells. Furthermore, TM directly promotes the proliferation of vascular smooth muscle cells, whereas recombinant TM (TMD123) containing the entire extracellular domain of TM inhibits the effect of TM on vascular smooth muscles. These studies suggest that TM plasma levels correlate with the degree of atherosclerosis and that soluble TM might reflect the severity of endothelial damage and associated inflammation in patients with atherosclerosis.[25] However, current research has focused on the correlation between TM and the pathological phenotype of atherosclerosis, and studies on the mechanism of TM involvement in the occurrence and development of atherosclerosis are relatively scarce. The discovery of non-coding RNAs (ncRNAs), including (miRNAs), long non-coding RNAs, and circular RNAs, and their roles in critical mechanisms of mRNA and protein expression, has sparked interest in their potential roles in atherosclerosis.[26]

Therefore, we further explored the action mechanism of TM in atherosclerosis. To better understand the pathogenesis of atherosclerosis and determine the underlying mechanism, we elucidated the role of the miR-550a-3p/TM axis in atherosclerosis by predicting the miRNAs upstream of TM. This study provides scientific evidence for the use of early diagnostic biomarkers and novel therapeutic targets for atherosclerosis.

Materials and Methods

Cell culture and establishment of cellular atherosclerosis model

Human vascular smooth muscle cells (HVSMCs) were obtained from the American Type Culture Collection (ATCC, USA). The HVSMCs were maintained in Dulbecco's modified Eagle medium (DMEM) (Gibco, Rockville, MD, USA) containing 10% foetal bovine serum (FBS) (Gibco) at 37°C in humid air under 5% CO_2 conditions. According to previous reports, HVSMCs were treated with ox-LDL (100 μg/mL) for 24 h to establish an atherosclerotic model.[27] Cell morphology was observed under an optical microscope (Olympus, Tokyo, Japan). The criterion for cellular atherosclerosis models was the formation of foam cell.[28] Lipid vacuoles were observed under a light microscope.

Dual-luciferase assay

A Dual-Luciferase Reporter Assay System Kit (Promega, Madison, WI, USA) was used to detect luciferase activity. The vector of the wild-type group was constructed by inserting a luciferase reporter vector with the sequence of the TM 3′-UTR containing the wild type miR-550a-3p-binding site. The luciferase vector harbours a mutant miR-550a-3p-binding site. A luciferase vector harbouring the TM 3′-UTR without the miR-550a-3p binding site was also constructed. Damaged HVSMCs were treated with luciferase reporter vectors and miR-550a-3p mimics using Lipofectamine 2000 (Invitrogen, Carlsbad, CA, USA), and luciferase activity was detected.

Cell counting kit-8 (CCK8) assay

The CCK8 assay kit was purchased from Beyotime Biotechnology (BL001B500T, Haimen, China). The cells were divided into normal control overexpression plasmid transfection (NC-OE), TM gene overexpression plasmid transfection (TM-OE), NC-mimics, hsa-miR-550a-3p-mimics, and TM-OE + hsa-miR-550a-3p-mimics with 3-5 replicates per group (approximately 2000 cells/well). The cell suspension (100 μL) was seeded into a 96-well plate. The culture plates were precultured in an incubator for 24 h (37°C, 5%CO_2). Different concentrations of substances (10 μL) were added to the culture plate. After incubating the culture plate in an incubator for 24 h, CCK8 solution (10 μL) was added to each well. The culture plate was incubated in an incubator for 1-4 h. The absorbance at 450 nm was measured using a microplate reader (Infinite F50, Tecan).

EDU (5-ethynyl-2-deoxyuridine) assay

Cell proliferation was evaluated using an EDU incorporation assay (Beyotime, Shanghai, China). Cells were treated with 100 μg/mL ox-LDL for 24 h and grouped as described earlier. The cells were then digested and seeded into 96-well plates at a density of 2×10^3 cells/well. Cells were cultured with 20 μM EdU diluent at 37°C and 5% CO_2 for 2 h. The cells were then fixed with 4% paraformaldehyde for 15 min. After washing the cells with phosphate-buffered saline (PBS), 1 mL of permeation solution was added to each well and incubated at room temperature for 15 min. Cells were incubated with endogenous peroxidase blocking solution at room temperature for 20 min and washed thrice with PBS. Click reaction solution (50 μL) was added to each well and incubated in darkness at room temperature for 30 min. The cells were then washed thrice with PBS. Streptavidin-hrp (STREptavin-HRP) working solution was added, incubated at room temperature for 30 min,

and then washed thrice with PBS. Subsequently, 0.1 mL TMB colour solution was added and incubated for 30 min at room temperature. The absorbance was measured at 370 nm.

Wound scratch assay

Before the operation, all instruments were sterilised, and the ruler was irradiated with ultraviolet light for 30 min. First, two horizontal lines were drawn on the back of the 12-well plate. HVSMCs (1.5×10^5 cells) were seeded into the wells. The Opti-MEM (31985070, Gibco) medium was changed the next day. The cells were rinsed gently with PBS 2-3 times, a low-concentration serum medium (0.5% FBS) was added, and images were captured. The cells were incubated at 37°C in a 5% CO_2 incubator, and images were captured on a fluorescence microscope at 12 h and 24 h after incubation (taking the shadow area in the centre of the 12-well as a reference, and the scratch was in the middle of the picture). The cell migration rate of each group was calculated according to the images obtained at 0, 16, and 24 h after scratching.

Transwell assay for invasion and migration

The 8-μm transwell kit was purchased from Millipore (Billerica, MA, USA). The required number of chambers was placed in a new 24-well plate for the migration experiments, and serum-free medium (100 μL) was added to the upper chamber. The cells were placed in a 37°C incubator for 1 h. Serum-free cell suspensions were prepared and counted. The number of cells was adjusted according to the pre-experiment; in general, 1×10^5 HVSMCs were seeded per well (24-well plate). The medium was carefully removed from the upper chamber, and 100 μL serum-free Dulbecco's modified Eagle medium (DMEM, C11965500BT; Gibco) was added. Next, 600 μL of 30% FBS (A3160802; Gibco) was added to the lower chamber. After incubating at 37°C for 48 h, the chamber was inverted on an absorbent paper to drain the medium completely. The non-transferred cells were gently removed from the chamber with a cotton swab, and 2-3 drops of crystal violet solution were dropped on the lower surface of the membrane to stain the transferred cells and incubated for 15 min. The chamber was then soaked for 15 min. A microscope was used to capture images. The field of view was randomly selected for each transwell chamber. Images were taken at 100× magnification, and the number of stained cells was counted. The experiment was repeated thrice. In the invasion experiments, Matrigel (BD, Franklin Lakes, NJ, USA) was coated on the upper chamber, and the other steps were the same as for the migration experiments.

Flow cytometer assay for cell cycle

When the HVSMCs in each experimental group grew to approximately 80% coverage, they were digested with trypsin and resuspended in DMEM to form a cell suspension. The cells were collected in a 5 mL centrifuge tube. Three replicate wells were set up for each group (cell number $\geq10^6$/dish). The samples were centrifuged at 1300 rpm for 5 min, and the supernatant was discarded. The cell pellet was washed once with PBS pre-cooled at 4°C. After centrifugation, the cells were fixed in 75% ethanol pre-cooled at 4°C for at least 1 h. Subsequently, 40× propidium iodide (PI) stock solution (2 mg/mL) and 100× RNase stock solution (10 mg/mL) were prepared. The volume of cell staining solution (0.6-1 mL) was adjusted according to the cell density, added to resuspend the cells, and analysed by flow cytometry (BD FACSCanto™; BD Biosciences, Franklin Lakes, NJ, USA).

Flow cytometer assay for cell apoptosis

When the cells in the six-well plate of each experimental group reached up to 80% confluence, the cells were digested with trypsin and then resuspended in a serum-free medium, which was collected in the same 5 mL centrifuge tube with the supernatant cells. Each group had three double pores (cell number $\geq5\times10^5$/well). After centrifugation at 1300 rpm for 5 min, the supernatant was discarded, and the cells were washed with D-Hanks solution (pH 7. 2-7.4) pre-cooled at 4°C. The cells were washed with 1× binding buffer by centrifuging at 1300 rpm for 3 min, and the cells were collected. The cell precipitate was resuspended in 1× binding buffer (200 μL) and stained with 2 μL annexin V-APC and PI for 20–60 min at room temperature. Finally, the cells were analysed using flow cytometry (BD FACSCanto™; BD Biosciences).

Real-time PCR

Real-time PCR was used to detect the expression of miR-550a-3p in HVSMCs. miRNAs were extracted using the PureLink® miRNA Isolation Kit (K1570-01, Thermo Fisher Scientific, Waltham, MA, USA). MiR-550a-3p expression was detected using SuperScript™ III Reverse Transcriptase (18080085, Thermo Fisher Scientific). U6 was used as an internal control. Each sample was analysed thrice, and the relative expression level of each gene was determined using the $2^{-\Delta\Delta CT}$ method. Primers for miR-550a-3p and U6 were synthesised by Sangon Biotechnology Co., Ltd. (Shanghai, China). The detailed methods of reverse transcription and amplification reactions have been described in a previous study.[29] Gene-specific primers used in this study are listed in Table S1.

Western blotting

Western blotting (WB) was used to detect the THBD protein expression in HVSMCs (GAPDH was used as the internal reference). The protein concentration in the foetal brain tissue was 4 μg/μL. An aliquot (15 μL) of the sample was added to a preconfigured 10% polyacrylamide gel (SDS-PAGE) for electrophoresis. The proteins were then transferred to polyvinylidene fluoride (PVDF) membranes. The membrane was blocked with 5% Tris-buffered saline with Triton X-100 (TBST) milk for 1.5 h and then washed thrice with distilled water for 5 min each. Primary and secondary antibody incubations were performed overnight at 4°C. After washing, an automatic exposure system (Tanon 1600; Shanghai Tianneng, China) was used to detect the target protein band. Details of the antibodies used are listed in Table S2.

Statistical analysis

All experimental data were analysed using the SPSS software v. 23.0 (SPSS Inc., Chicago, IL, USA). The results are expressed as mean ± standard error of the mean (SEM). The experimental results of multiple groups were compared using one-way analysis of variance (ANOVA). If the analysis of variance was significant, further pairwise comparisons were made, and the Student-Newman-Keuls q (SNK) test was used. Student's *t*-tests were used to compare two groups. A value of $p<0.05$ was considered statistically significant.

Results

Ox-LDL induces HVSMC injury to establish an atherosclerotic cell model

To establish an atherosclerotic cell model, ox-LDL (100 μg/mL) was used to induce HVSMC injury. After 24 h, the cell morphology was observed under a microscope. Compared to that in the control group (0 μg/mL ox-LDL), HVSMCs morphology were damaged, lipid vacuoles could be found in the 100 μg/mL ox-LDL group (Figure 1A). The results of RT-PCR revealed that the expression level of the TM gene in the 24 h group was lower than that in the 0 h group (Figure 1B; $p<0.01$). Further, the apoptosis rate of the 100 μg/mL ox-LDL group was increased (Figure 1 C,D; $p<0.01$). The WB results showed that the TM protein levels in the 20, 40, 60, 80, and 100 μg/mL ox-LDL-treated groups were lower than that in the control group (0 μg/mL ox-LDL group); the expression level in the 100 μg/mL ox-LDL group was the lowest (Figure 1 E,F; $p<0.01$). These results collectively indicate that 100 μg/mL ox-LDL induced HVSMC injury, and an atherosclerotic cell model was successfully established.

MiR-550a-3p is a direct target of TM

By predicting the miRNAs upstream of TM, we observed that miR-550a-3p had the highest binding score with TM according to the database prediction. MiR-550a-3p was found to be a predicted target of TM (Figure 2A). Hsa-miR-550a-3p reduced the activity of the TM-3′-UTR by 17% compared to that in the normal control group (NC; **p<0.01). The results suggested that hsa-miR-550a-3p acted on the TM-3′-UTR region. Mutating the TM-3′-UTR region increased its activity by 32.5% compared to that of the wild-type (Figure 2B; **p<0.01). These results indicated that the mutation site was the site of interaction. RT-PCR results revealed that, compared to that in the NC, the expression level of hsa-miR-550a-3p was increased in the hsa-miR-550a-3p mimics group (Figure 2C; **p<0.01). In contrast, the expression level of the TM gene was decreased (Figure 2D; **p<0.01).

Expression of miR-550a-3p/THBD axis affects cell proliferation in atherosclerosis

We used CCK8 and BrdU assays to detect the effect of the miR-550a-3p/TM axis on the proliferation of HVSMCs. The results of the CCK8 assay suggested that cell proliferation in the TM-OE group was accelerated compared to that in the control NC-OE group (p<0.01). Compared to that in the NC mimics group, the proliferation of the hsa-miR-550a-3p-mimics group was reduced (p<0.01). After transfection with the TM gene overexpression plasmid and hsa-miR-550a-3p mimic, the cell proliferation rate in the TM-OE+hsa-miR-550a-3p-mimics group recovered to a level similar to that in the control group (Figure 3A). The results of the BrdU assay were consistent with that of the CCK8 assay (Figure 3B).

Expression of miR-550a-3p/TM axis affects cell migration and invasion in atherosclerosis

We used scratch and transwell assays to examine the effect of the miR-550a-3p/TM axis on the migration function of HVSMCs. The results suggested that the transwell mobility of the TM-OE group was higher than that of the control NC-OE group (**p<0.01). Compared to that in the NC mimics group, the transwell mobility of the hsa-miR-

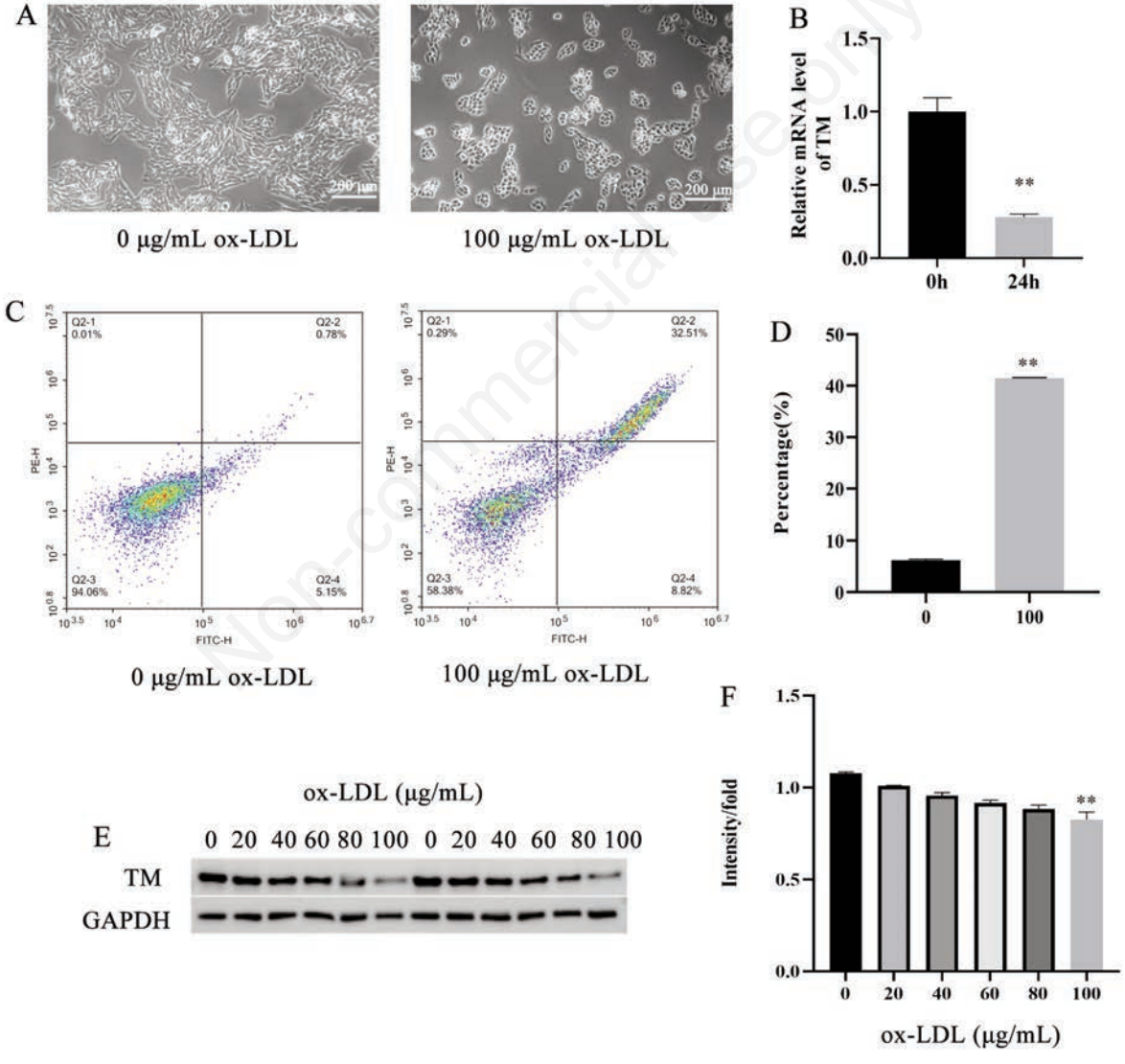

Figure 1. Ox-LDL induces human vascular smooth muscle cell (HVSMC) injury to establish an atherosclerotic cell model. A) HVSMCs were treated with different concentrations of ox-LDL; arrows pointed the lipid vacuoles. B) TM mRNA levels. C) Cell apoptosis rate (%). D) Flow cytometry analysis of apoptosis in HVSMCs after treatment with different concentrations of ox-LDL. E) TM immunoluminescence bands. F) TM protein levels.

550a-3p-mimics group was decreased (**p<0.01). After TM gene overexpression plasmid transfection and hsa-miR-550a-3p mimics transfection, the transwell mobility of the TM-OE+hsa-miR-550a-3p-mimics group recovered to a level similar to that of the control group. The scratch assay results were consistent with that of the transwell assay (Figure 4 A,B,D,E). Furthermore, we used the transwell assay to examine the effect on the invasive function of HVSMCs. Compared to that in the NC-OE group, the invasion and metastasis rate in the TM-OE group increased (**p<0.01); compared to that in the NC-mimics group, the invasion and metastasis rate of hsa-miR-550a-3p-mimics group decreased (**p<0.01). After transfection with the TM gene overexpression plasmid and hsa-miR-550a-3p mimics, the invasion and metastasis rates of the TM-OE+hsa-miR-550a-3p-mimics group recovered to the same level as the control groups (Figure 4 C,F).

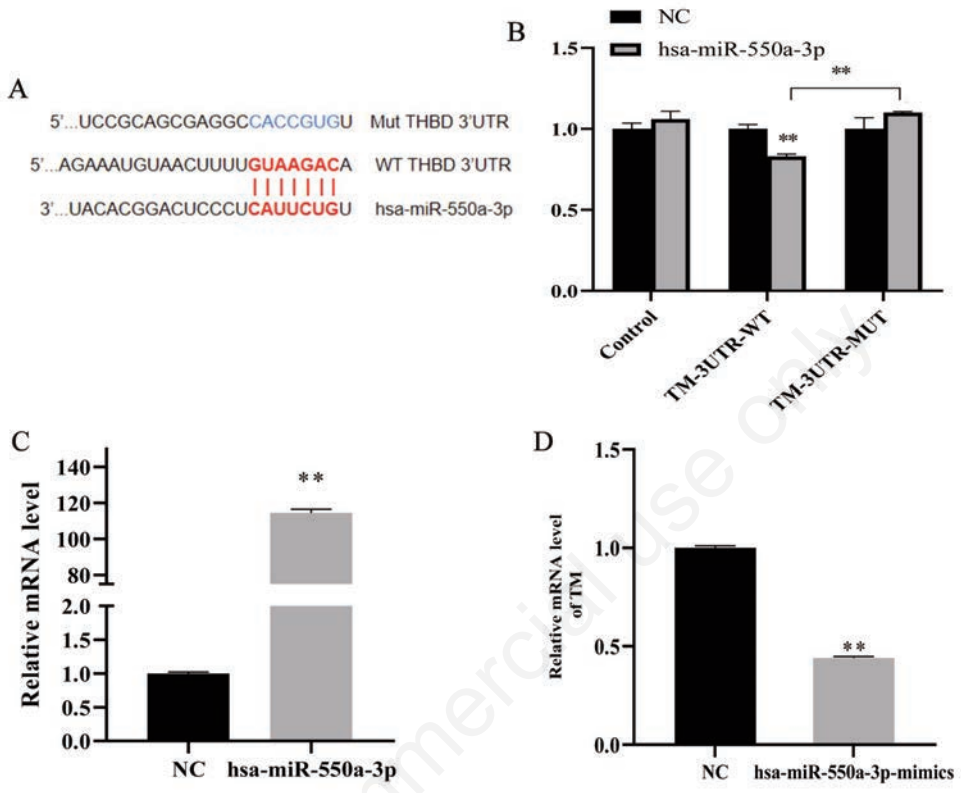

Figure 2. **miR-550a-3p is a direct target of TM. A) The predicted binding sites of miR-550a-3p in the 3′-UTR of TM. B) Dual-luciferase reporter assay was used to determine the binding site. C) The hsa-miR-550a-3p mRNA level and (D) TM mRNA level.**

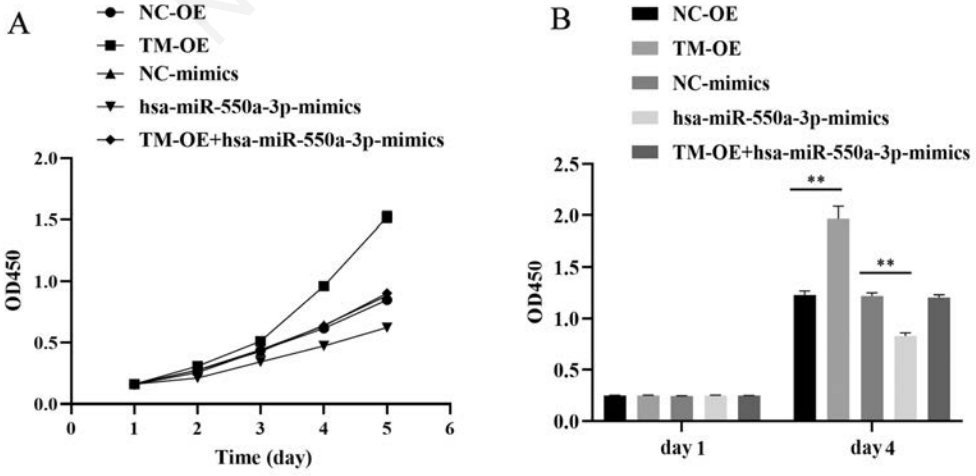

Figure 3. **Expression of miR-550a-3p/TM axis affects cell proliferation in atherosclerosis. CCK8 (A) and BrdU (B) assays were performed to determine the proliferation of HVSMCs.**

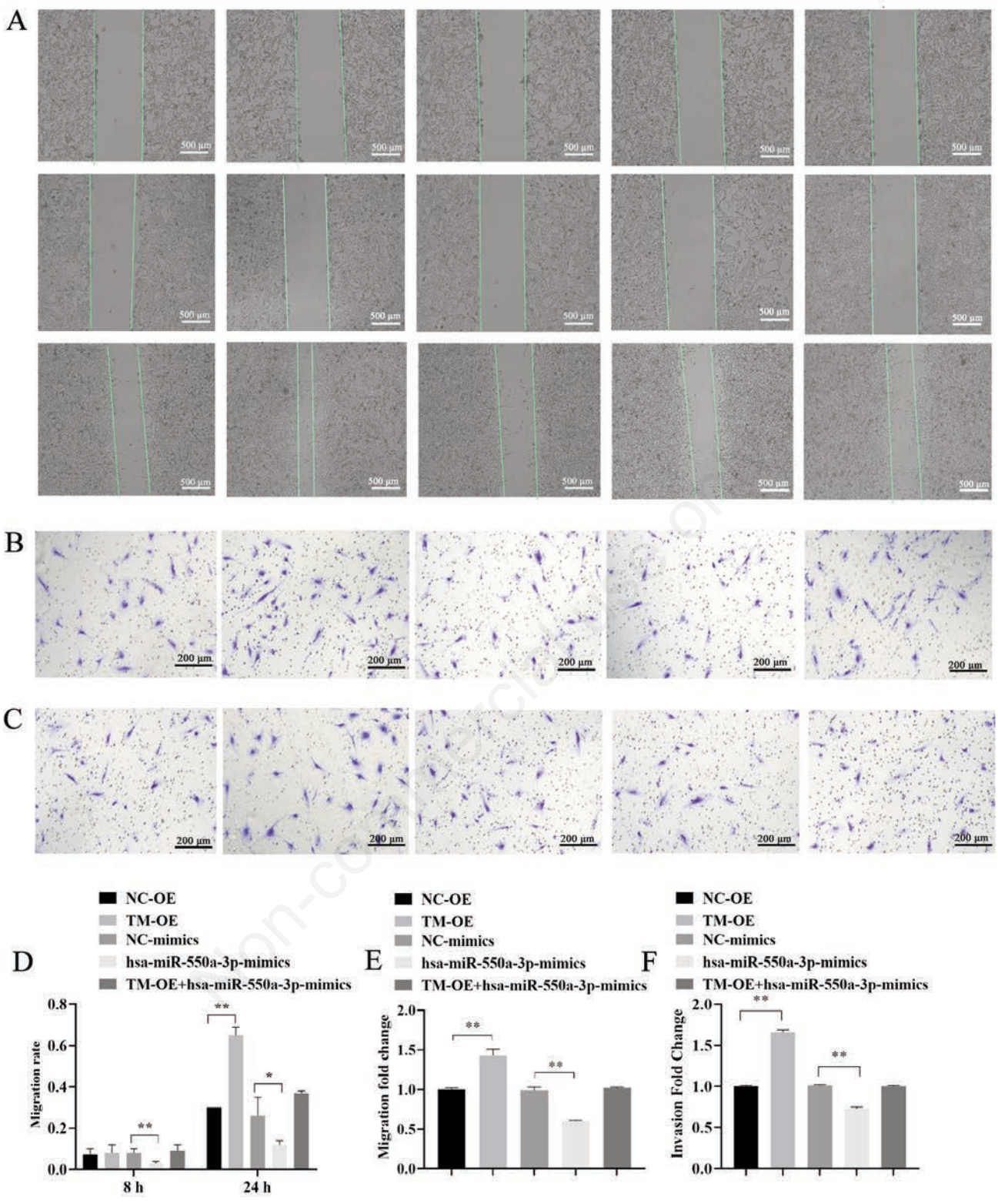

Figure 4. Expression of miR-550a-3p/TM axis affected cell migration in atherosclerosis. Scratch (A) and transwell (B) assays were performed to determine the migration of HVSMCs. C) Transwell assay was performed to determine invasion of HVSMCs. D) Migration rate. E) Migration fold change. F) Invasion fold change.

Expression of the miR-550a-3p/TM axis affects the cell cycle in atherosclerosis

We used the PI-FACS assay to detect the effect of the miR-550a-3p/TM axis on the cell cycle of HVSMCs. Compared to that in the NC-OE group, the TM-OE group had fewer cells in the G_1 phase (**p<0.01) and more cells in the S phase (**p<0.01). No significant differences were observed in the number of cells in the G_2/M phase. Compared to that in the NC mimics group, the hsa-miR-550a-3p-mimics group had more cells in the G_1 phase (**p<0.01) and fewer cells in the S and G_2/M phases (**p<0.01). After TM gene overexpression plasmid transfection and hsa-miR-550a-3p gene mimic transfection, no significant difference was observed in cells in the G_1, S, and G_2/M phases in the TM-OE+hsa-miR-550a-3p-mimics group (Figure 5A).

Expression of miR-550a-3p/TM axis affected cell apoptosis in atherosclerosis

The double-stained cell apoptosis detection results suggested that the apoptosis rate in the TM-OE group was lower than that in the NC-OE group (*p<0.05). Compared to the NC mimics group, the apoptosis rate of the hsa-miR-550a-3p-mimics group was increased (**p<0.01). After transfection of the TM gene overexpression plasmid and hsa-miR-550a-3p gene mimics, the apoptosis rate of the TM-OE+hsa-miR-550a-3p-mimics group recovered to a level similar to that of the control group (Figure 6A).

Discussion

TM is involved in the pathological process of atherosclerosis.[30] For example, TM inhibits the action of thrombin by binding to thrombin through TM domains 2 and 3 (TMD23).[31,32] The recombinant TMD23 (rTMD23) protein significantly reduced atherosclerosis and neointimal formation through its thrombin-binding ability. rTMD23 protein can effectively reduce the activation of protease-activated receptor-1 (PAR-1) by binding to thrombin and downregulating the activation of downstream signals of PAR-1.[33] PAR-1 activation-induced cellular effects, such as endothelial permeability, adhesion molecule expression, and cytokine production, were also reduced following rTMD23 treatment.[34] However, the potential mechanism of TM in atherosclerosis has not yet been elucidated. In our study, we successfully induced a model of atherosclerosis using vascular endothelial cells and observed decreased expression level of TM in injured vascular endothelial cells. These

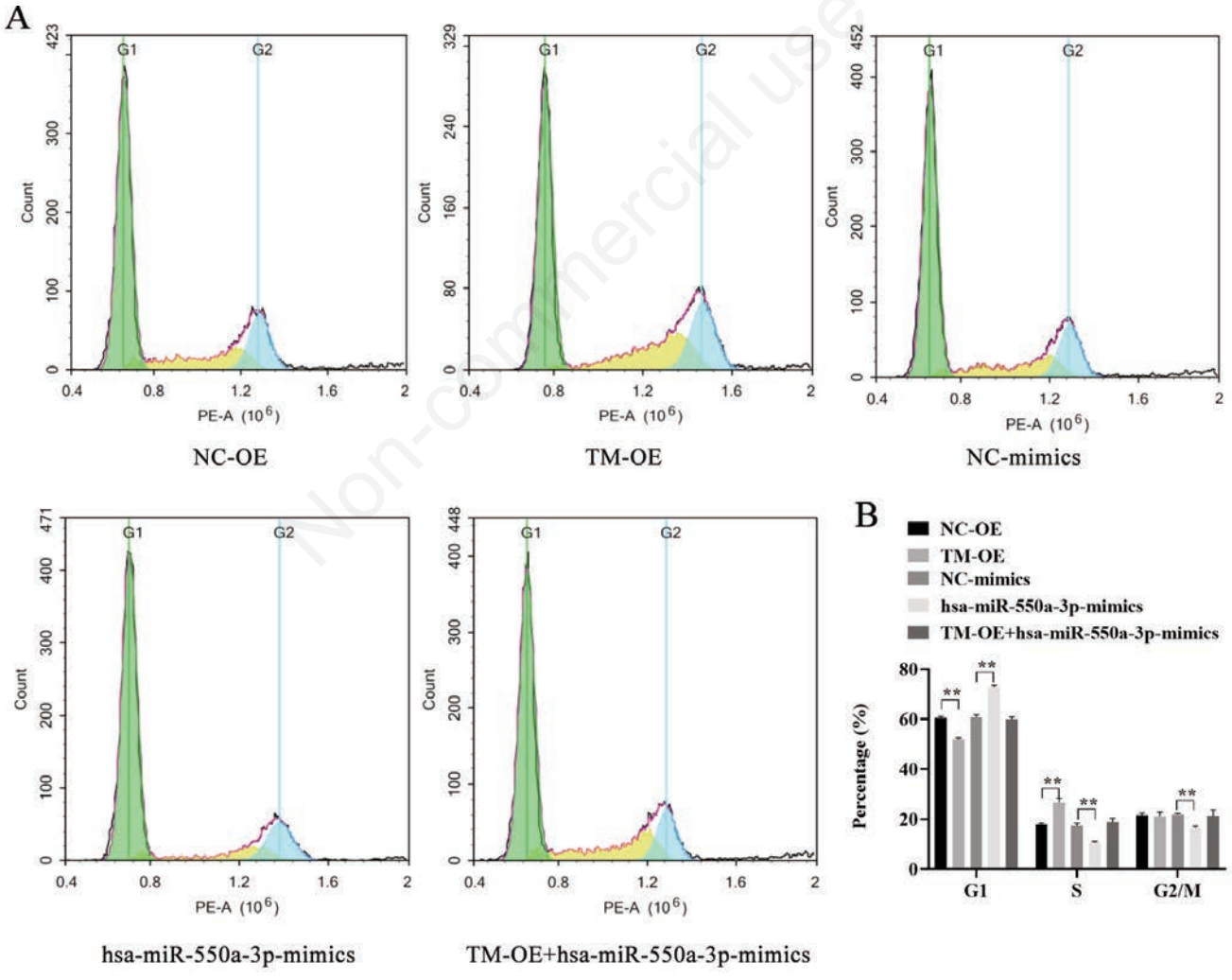

Figure 5. Expression of miR-550a-3p/TM axis affected the cell cycle in atherosclerosis. NC-OE, TM-OE, NC-mimics, Hsa-miR-550a-3p, and TM-OE+hsa-miR-550a-3p mimics cell cycles (A). B) Cell cycle percentage.

results collectively suggest that TM is a diagnostic biomarker for atherosclerosis. To further explore the potential action mechanism of TM in atherosclerosis, we investigated potential targets of TM. By predicting the miRNAs upstream of TM, we identified that miR-550a-3p was the direct upstream target of TM. miRNAs belong to the family of non-coding RNAs, 18-25 nucleotides in length, and inhibit the translation of specific target genes by directly binding to the 3′-UTR of mRNA.[35,3] In a recent study, miR-550a-3p has been confirmed to be involved in the pathological progression of various diseases. For example, miR-550a-3p has been associated with different types of tumours, including breast cancer, lung adenocarcinoma, colorectal cancer, and hepatocellular carcinoma.[37-39] Furthermore, circulating miR-550a-3p might serve as a biomarker for severe acute pancreatitis associated with Alzheimer's disease and acute lung injury.[40,41] miR-550a-3p circulation was also significantly altered in patients with osteoporosis and fragility fractures who were idiopathic and postmenopausal.[42] In patients with diabetes, miRNA-550a interferes with vitamin D metabolism in peripheral B cells.[43] However, the specific function of miR-550a-3p in atherosclerosis has not yet been elucidated.

We also performed gain-and-loss experiments to investigate the mechanism by which the miR-550a-3/TM axis affects atherosclerosis progression. We observed that upregulation of miR-550a-3p levels significantly reduced the proliferation of HVSMCs, whereas overexpression of TM significantly promoted its growth. After transfection with the TM gene overexpression plasmid and hsa-miR-550a-3p mimics, the proliferation of HVSMCs returned to normal levels, which provided a new target for the treatment of atherosclerosis. Since vascular endothelial cell migration and invasion are correlated with atherosclerosis, we next demonstrated that the miR-550a-3p/TM axis could restore the normal invasion and migration capabilities of damaged HVSMCs.[44] Further studies revealed that the miR-550a-3p/TM axis could regulate apoptosis and the cell cycle of damaged HVSMCs. Our data provide a potential biological basis for the effective treatment of atherosclerosis. To verify whether miR-550a-3p is a functional target of TM, we performed a dual-luciferase assay in HVSMCs. In addition, TM protein levels were detected in miR-550a-3p knockdown cells, and miR-550a-3p was negatively correlated with TM protein levels. Meanwhile, overexpression of TM by miR-550a-3p reversed the effect of the mimic, which further confirmed that miR-550a-3p repaired the proliferation, invasion, migration, and apoptosis of damaged HVSMCs through TM and altered their cell cycle. However, in this study, we targeted only miR-550a-3p, which has limitations in the molecular mechanism of

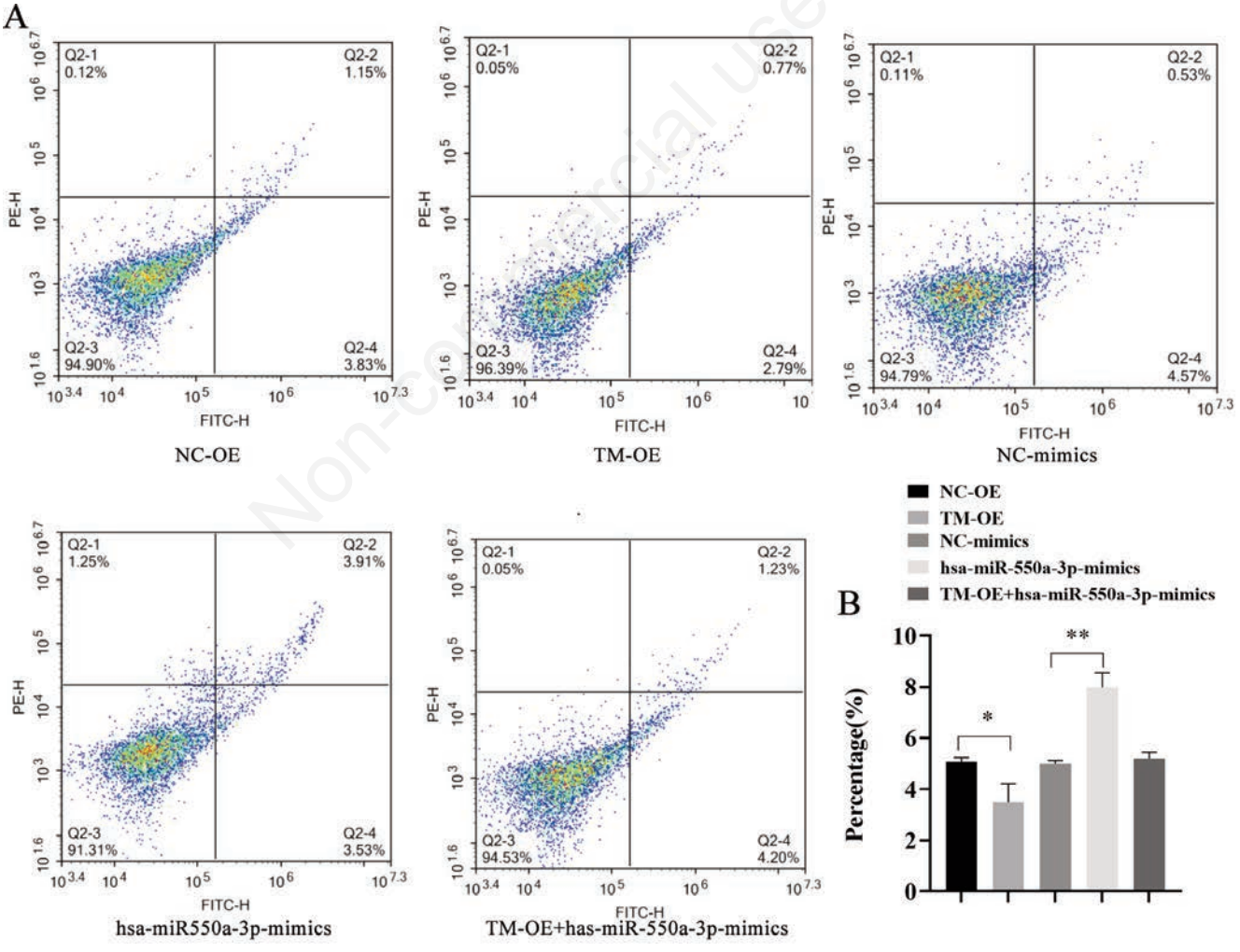

Figure 6. Expression of miR-550a-3p/TM axis affected cell apoptosis in atherosclerosis. Flow cytometry analysis of apoptosis in NC-OE, TM-OE, NC-mimics, Hsa-miR-550a-3p, and TM-OE+hsa-miR-550a-3p (A). B) Cell apoptosis percentage.

TM. Since the miRNA regulatory mechanism is a network system,[26] one miRNA can target different genes, and one gene can be regulated by different miRNAs. However, further animal studies are required to validate our results. Our study is the first to demonstrate the function of the miR-550a-3/TM axis in atherosclerosis and partially elucidate miR-550a-3p as a target gene involved in TM regulatory mechanisms.

In summary, miR-550a-3p may play a role in atherosclerosis, and for the first time, we normalised the function of injured vascular endothelial cells by simultaneous transfection of TM and miR-550a-3p. These results suggest that the miR-550a-3p/TM axis is a potential therapeutic target for atherosclerosis.

References

1. Libby P, Bornfeldt KE, Tall AR. Atherosclerosis: Successes, surprises, and future challenges. Circ Res 2016;118:531-4.
2. Herrington W, Lacey B, Sherliker P, Armitage J, Lewington S. Epidemiology of atherosclerosis and the potential to reduce the global burden of atherothrombotic disease. Circ Res 2016;118:535-46.
3. Tedgui A, Mallat Z. Cytokines in atherosclerosis: pathogenic and regulatory pathways. Physiol Rev 2006;86:515-81.
4. Falk E. Pathogenesis of atherosclerosis. J Am Coll Cardiol 2006;47:C7-12.
5. Hansson GK, Hermansson A. The immune system in atherosclerosis. Nat Immunol 2011;12:204-12.
6. Libby P. The changing landscape of atherosclerosis. Nature 2021;592:524-33.
7. Zhu Y, Xian X, Wang Z, Bi Y, Chen Q, Han X, et al. Research progress on the relationship between atherosclerosis and inflammation. Biomolecules 2018;8:80.
8. Chen PS, Wang KC, Chao TH, Chung HC, Tseng SY, Luo CY, et al. Recombinant thrombomodulin exerts anti-autophagic action in endothelial cells and provides anti-atherosclerosis effect in apolipoprotein E deficient mice. Sci Rep 2017;7:3284.
9. Qian G, Ding Z, Zhang B, Li Q, Jin W, Zhang Q. Association of thrombomodulin Ala455Val dimorphism and inflammatory cytokines with carotid atherosclerosis in the Chinese Han population. J Inflamm Res 2012;5:117-23.
10. Raife TJ, Dwyre DM, Stevens JW, Erger RA, Leo L, Wilson KM, et al. Human thrombomodulin knock-in mice reveal differential effects of human thrombomodulin on thrombosis and atherosclerosis. Arterioscler Thromb Vasc Biol 2011;31:2509-17.
11. Wei Y, Lai B, Liu H, Li Y, Zhen W, Fu L. Effect of cigarette smoke extract and nicotine on the expression of thrombomodulin and endothelial protein C receptor in cultured human umbilical vein endothelial cells. Mol Med Rep 2018;17:1724-30.
12. Martinez-Fierro ML, Castruita-De La Rosa C, Garza-Veloz I, Cardiel-Hernandez RM, Espinoza-Juarez MA, Delgado-Enciso I, et al. Early pregnancy protein multiplex screening reflects circulating and urinary divergences associated with the development of preeclampsia. Hypertens Pregnancy 2018;37:37-50.
13. Rega-Kaun G, Kaun C, Ebenbauer B, Jaegersberger G, Prager M, Wojta J, et al. Bariatric surgery in morbidly obese individuals affects plasma levels of protein C and thrombomodulin. J Thromb Thrombolysis 2019;47:51-6.
14. Loghmani H, Conway EM. Exploring traditional and nontraditional roles for thrombomodulin. Blood 2018;132:148-58.
15. Tucker EI, Verbout NG, Markway BD, Wallisch M, Lorentz CU, Hinds MT, et al. The protein C activator AB002 rapidly interrupts thrombus development in baboons. Blood 2020;135:689-99.
16. O'Donnell JS, O'Sullivan JM, Preston RJS. Advances in understanding the molecular mechanisms that maintain normal haemostasis. Br J Haematol 2019;186:24-36.
17. Stojanovski BM, Pelc LA, Zuo X, Di Cera E. Zymogen and activated protein C have similar structural architecture. J Biol Chem 2020;295:15236-44.
18. Lee C, Viswanathan G, Choi I, Jassal C, Kohlmann T, Rajagopal S. Beta-arrestins and receptor signaling in the vascular endothelium. Biomolecules 2020;11:9.
19. Lymperopoulos A. Arrestins in the cardiovascular system: an update. Prog Mol Biol Transl Sci 2018;159:27-57.
20. Sebert M, Sola-Tapias N, Mas E, Barreau F, Ferrand A. Protease-activated receptors in the intestine: focus on inflammation and cancer. Front Endocrinol (Lausanne) 2019;10:717.
21. Gianazza E, Brioschi M, Baetta R, Mallia A, Banfi C, Tremoli E. Platelets in healthy and disease states: from biomarkers discovery to drug targets identification by proteomics. Int J Mol Sci 2020;21:4541.
22. Li J, Hara H, Wang Y, Esmon C, Cooper DKC, Iwase H. Evidence for the important role of inflammation in xenotransplantation. J Inflamm (Lond) 2019;16:10.
23. Laszik ZG, Zhou XJ, Ferrell GL, Silva FG, Esmon CT. Down-regulation of endothelial expression of endothelial cell protein C receptor and thrombomodulin in coronary atherosclerosis. Am J Pathol 2001;159:797-802.
24. Tohda G, Oida K, Okada Y, Kosaka S, Okada E, Takahashi S, et al. Expression of thrombomodulin in atherosclerotic lesions and mitogenic activity of recombinant thrombomodulin in vascular smooth muscle cells. Arterioscler Thromb Vasc Biol 1998;18:1861-9.
25. Li J, Garnette CS, Cahn M, Claytor RB, Rohrer MJ, Dobson JG Jr., et al. Recombinant thrombomodulin inhibits arterial smooth muscle cell proliferation induced by thrombin. J Vasc Surg 2000;32:804-13.
26. Fasolo F, Di Gregoli K, Maegdefessel L, Johnson JL. Non-coding RNAs in cardiovascular cell biology and atherosclerosis. Cardiovasc Res 2019;115:1732-56.
27. Yuan L, Wang D, Wu C. Protective effect of liquiritin on coronary heart disease through regulating the proliferation of human vascular smooth muscle cells via upregulation of sirtuin1. Bioengineered. 2022;13:2840-50.
28. Llorente-Cortés V, Martínez-González J, Badimon L. LDL receptor-related protein mediates uptake of aggregated LDL in human vascular smooth muscle cells. Arterioscler Thromb Vasc Biol 2000;20:1572-9.
29. Yu Z, Han Y, Shen R, Huang K, Xu YY, Wang QN, et al. Gestational di-(2-ethylhexyl) phthalate exposure causes fetal intrauterine growth restriction through disturbing placental thyroid hormone receptor signaling. Toxicol Lett 2018;294:1-10.
30. Li YH, Shi GY, Wu HL. The role of thrombomodulin in atherosclerosis: from bench to bedside. Cardiovasc Hematol Agents Med Chem 2006;4:183-7.
31. Giri H, Cai X, Panicker SR, Biswas I, Rezaie AR. Thrombomodulin regulation of mitogen-activated protein kinases. Int J Mol Sci 2019;20:1851.
32. Pai VC, Lo IC, Huang YW, Tsai IC, Cheng HP, Shi GY, et al. The chondroitin sulfate moiety mediates thrombomodulin-enhanced adhesion and migration of vascular smooth muscle cells. J Biomed Sci 2018;25:14.
33. Wei HJ, Li YH, Shi GY, Liu SL, Chang PC, Kuo CH, et al. Thrombomodulin domains attenuate atherosclerosis by inhibiting thrombin-induced endothelial cell activation. Cardiovasc Res 2011;92:317-27.
34. Li YH, Kuo CH, Shi GY, Wu HL. The role of thrombomodulin lectin-like domain in inflammation. J Biomed Sci 2012;19:34.
35. Adams BD, Parsons C, Walker L, Zhang WC, Slack FJ. Targeting noncoding RNAs in disease. J Clin Invest 2017;127:761-71.
36. Wu HH, Lin WC, Tsai KW. Advances in molecular biomarkers for gastric cancer: miRNAs as emerging novel cancer markers. Expert Rev Mol Med 2014;16:e1.

37. Ho JY, Hsu RJ, Wu CH, Liao GS, Gao HW, Wang TH, et al. Reduced miR-550a-3p leads to breast cancer initiation, growth, and metastasis by increasing levels of ERK1 and 2. Oncotarget 2016;7:53853-68.
38. Tian Q, Liang L, Ding J, Zha R, Shi H, Wang Q, et al. MicroRNA-550a acts as a pro-metastatic gene and directly targets cytoplasmic polyadenylation element-binding protein 4 in hepatocellular carcinoma. PLoS One 2012;7:e48958.
39. Wang G, Fu Y, Yang X, Luo X, Wang J, Gong J, et al. Brg-1 targeting of novel miR550a-5p/RNF43/Wnt signaling axis regulates colorectal cancer metastasis. Oncogene 2017;36:5915.
40. Lu XG, Kang X, Zhan LB, Kang LM, Fan ZW, Bai LZ. Circulating miRNAs as biomarkers for severe acute pancreatitis associated with acute lung injury. World J Gastroenterol 2017;23:7440-9.
41. Satoh J, Kino Y, Niida S. MicroRNA-Seq data analysis pipeline to identify blood biomarkers for Alzheimer's disease from public data. Biomark Insights 2015;10:21-31.
42. He J, Guo X, Liu ZQ, Yang PC, Yang S. Micro RNA-550a interferes with vitamin D metabolism in peripheral B cells of patients with diabetes. Cell Biochem Funct 2016;34:640-6.
43. Kocijan R, Muschitz C, Geiger E, Skalicky S, Baierl A, Dormann R, et al. Circulating microRNA signatures in patients with idiopathic and postmenopausal osteoporosis and fragility fractures. J Clin Endocrinol Metab 2016;101:4125-34.
44. Mozos I, Malainer C, Horbanczuk J, Gug C, Stoian D, Luca CT, et al. Inflammatory markers for arterial stiffness in cardiovascular diseases. Front Immunol 2017;8:1058.

Received for publication: 23 April 2022. Accepted for publication: 4 July 2022.

Licensee PAGEPress, Italy
European Journal of Histochemistry 2022; 66:3429
doi:10.4081/ejh.2022.3429